LATE HOLOCENE CHRONOLOGY OF SURFACE-FAULTING EARTHQUAKES AT THE CORNER CANYON SITE ON THE SALT LAKE CITY SEGMENT OF THE WASATCH FAULT ZONE, UTAH

Submitted by
Adam I. Hiscock[1] and Christopher B. DuRoss[1,2]
adamhiscock@utah.gov

With assistance from:

Greg N. McDonald[1], Michael D. Hylland[1], Scott E. K. Bennett[4], Steven F. Personius[3], Ryan D. Gold[3], Richard W. Briggs[3], Nadine G. Reitman[3], Joshua D. Devore[5], and Shannon A. Mahan[6]

[1] Utah Geological Survey, Salt Lake City, Utah
[2] currently at U.S. Geological Survey, Golden, Colorado
[3] U.S. Geological Survey, Golden Colorado
[4] U.S. Geological Survey, Seattle, Washington
[5] Ohio State University, Dublin, Ohio
[6] U.S. Geological Survey, Denver, Colorado

December 1, 2016

CONTENTS

Figures

Figure 1. Salt Lake City and Provo segments of the Wasatch fault zone
Figure 2. Oblique east slope-shade map of the Traverse Mountains salient
Figure 3. Slope-shade maps of the Corner Canyon site
Figure 4. Scarp profile measured across the Corner Canyon site
Figure 5. Photo of Corner Canyon site and excavation
Figure 6. Photomosaic of the fault zone at the Corner Canyon site

Tables

Table 1. Correlation of surface-faulting earthquakes on the Salt Lake City segment
Table 2. Evidence for surface-faulting earthquakes at the Corner Canyon site

Appendices

Appendix A: Description of stratigraphic units at the Corner Canyon site
Appendix B: Radiocarbon ages for the Corner Canyon site
Appendix C: Optically stimulated luminescence ages for the Corner Canyon site

Plates[1]

Plate 1: Stratigraphic and structural relations in the south wall at the Corner Canyon trench site
Plate 2: Stratigraphic and structural relations in the north wall at the Corner Canyon trench site

[1] *Download a high-resolution version of this report at*
http://ugspub.nr.utah.gov/publications/non_lib_pubs/contract/G14AP00057.pdf

ABSTRACT

The Utah Geological Survey excavated a trench at the Corner Canyon site on the southern portion of the Salt Lake City segment (SLCS) of the Wasatch fault zone (WFZ) to improve estimates of Holocene surface-faulting earthquake timing, displacement, and rupture extent and to explore the potential for rupture across the segment boundary between the SLCS and adjacent Provo segment (PS). Paleoseismic data from the Corner Canyon site expand the Holocene record of earthquakes on the southern SLCS. Preliminary data indicate at least six surface-faulting earthquakes (youngest to oldest, CC1 to CC6) at the Corner Canyon site. Earthquakes CC6 to CC3 occurred between ~5 and 1 ka and correspond with previously identified earthquakes on the SLCS. Earthquakes CC2 and CC1 are younger than ~1 ka, postdating previously identified SLCS earthquakes. Additional analyses of these data and a comparison of the SLCS and PS earthquake records will improve our understanding of coseismic interactions between the central WFZ segments, as well as serving to improve and update probabilistic earthquake-hazard analyses for the Wasatch Front.

INTRODUCTION

Purpose and Scope

The Salt Lake City segment (SLCS) of the Wasatch fault zone (WFZ) extends along the base of the Wasatch Range in Salt Lake Valley, which has a population of over 1 million residents and faces the greatest earthquake risk in the Intermountain West. The SLCS comprises three subsections—the Warm Springs, East Bench, and Cottonwood faults (figure 1)—that extend for about 40 km and have abundant evidence of large-magnitude (M ~7), surface-faulting earthquakes in the latest Pleistocene and Holocene (Personius and Scott, 1992; Machette and others, 1992; Lund, 2005; Working Group on Utah Earthquake Probabilities, 2016). Although the SLCS has been the subject of several paleoseismic trenching investigations (Swan and others, 1981; Schwartz and Lund, 1988; Black and others, 1996; McCalpin, 2002; DuRoss and Hylland, 2015), important questions remained at the time of this study regarding the timing and rupture extent of Holocene earthquakes on the segment. These uncertainties lead to complex models of fault segmentation and recurrence (e.g., WFZ rupture models summarized in Lund, 2010), which impact both seismic-hazard assessments (e.g., for the U.S. Geological Survey [USGS] National Seismic Hazard Maps) and earthquake-probability calculations (e.g., by the Working Group on Utah Earthquake Probabilities, 2016).

In June 2014, the Utah Geological Survey (UGS), in collaboration with the USGS, excavated a fault trench at the Corner Canyon site on the southernmost part of the Cottonwood fault. The purpose in developing additional paleoseismic data for the SLCS was to (1) reduce uncertainties in earthquake timing, recurrence, and displacement; (2) clarify the rupture extent of SLCS earthquakes; and (3) explore the potential for coseismic interactions between the SLCS and adjacent Provo segment (PS). Improving these fault and earthquake parameters is fundamental to modeling the seismic moment release and recurrence intervals of past earthquakes on the fault, and to updating seismic-hazard assessments for the Wasatch Front region.

Salt Lake City Segment of the Wasatch Fault Zone

The Holocene-active trace of the 40-km-long SLCS consists of three subsections separated by left steps: the Warm Springs, East Bench, and Cottonwood faults (Scott and Shroba, 1985; Personius and Scott, 1992) (figure 1). At the northern end of the SLCS, the 10-km-long Warm Springs fault marks the western edge of the Salt Lake salient, a fault-bounded block of Tertiary bedrock that defines the boundary between the SLCS and the Weber segment to the north. Because of extensive surface mining and development along the Warm Springs fault, limited paleoseismic data (and no suitable trench sites; DuRoss and others, 2014) exists. At the southern end of the Warm Springs fault, the SLCS steps east about 3–4 km to the East Bench fault. The East Bench fault is 12 km long and consists of large, prominent scarps that bound uplifted and incised alluvial-fan surfaces. The East Bench fault is also extensively developed and only has per-event timing and displacement data from a single site at the northern end of the fault (Penrose Drive site; DuRoss and others, 2014; figure 1). At the southern end of the East Bench fault, the SLCS steps 2–3 km eastward to the Cottonwood fault—a 20-km long, complex fault zone that generally follows the range front. Although the Cottonwood fault is extensively developed, paleoseismic data are available from investigations at two sites near the center of the fault (South Fork Dry Creek [Black and others, 1996] and Little Cottonwood Canyon [Swan and others, 1981; McCalpin, 2002]; figure 1). The Cottonwood fault extends to the southern end of the SLCS near Corner Canyon, where the Traverse Mountains and east-west oriented Fort Canyon fault (Bruhn and others, 1992) separate the SLCS from the 59-km long PS to the south (figure 1).
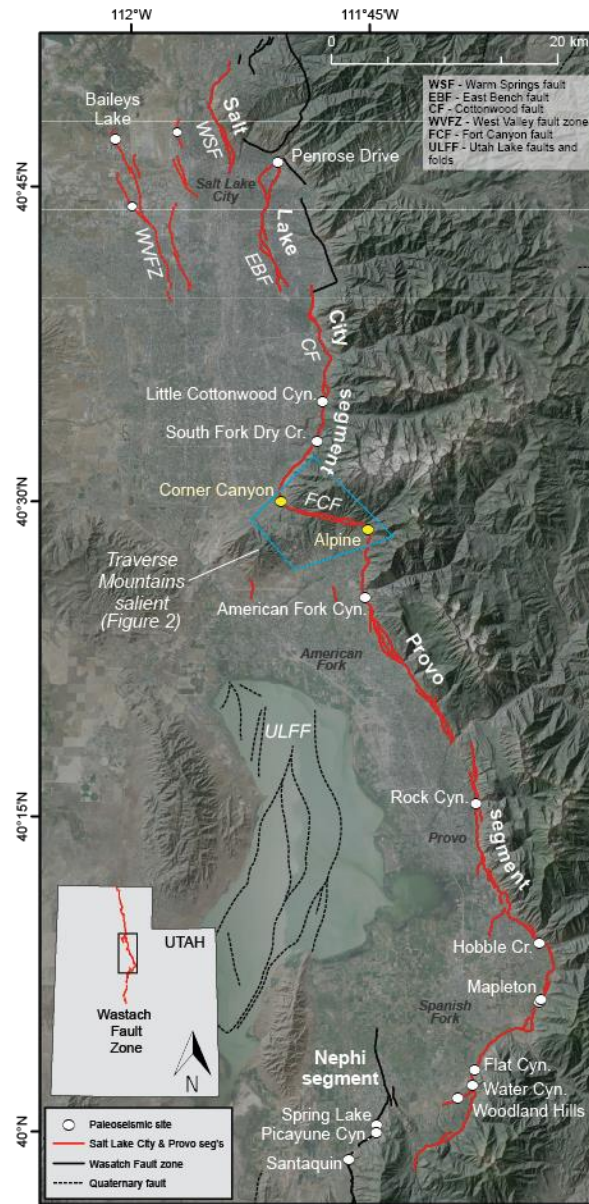
Figure 1. *Salt Lake City and Provo segments of the Wasatch fault zone in northern Utah. Subsections of the Salt Lake City segment are the Warm Springs fault (WSF), East Bench fault (EBF), and Cottonwood fault (CF). Corner Canyon and Alpine (Bennett and others, 2015) paleoseismic sites shown in yellow; other paleoseismic sites shown as white dots. Approximate outline of figure 2 shown in light blue. Fault traces are from the Utah Quaternary Fault and Fold Database (http://geology.utah.gov/resources/data-databases/qfaults/); base map created from 2011 NAIP imagery and USGS 10-m NED data.*

Previous paleoseismic data for the SLCS (table 1) are relatively limited because of extensive development along the fault. Earthquake-timing data are available for the Cottonwood and East Bench faults, but not the Warm Springs fault. At the Little Cottonwood Canyon site (figure 1), the Cottonwood fault vertically offsets latest Pleistocene glacial till and Lake Bonneville lacustrine sediments 22 m (Personius and Scott, 1992). McCalpin (2002) interpreted seven post-Bonneville (<18 ka) earthquakes, including four earthquakes younger than about 6 ka (table 1). About 5 km south of Little Cottonwood Canyon, Schwartz and Lund (1988) and Black and others (1996) excavated trenches at the South Fork Dry Creek site (figure 1), where the Cottonwood fault forms a complex zone of faulting in Holocene alluvial-fan deposits. Black and others (1996) established a chronology of four earthquakes since about 5.3 ka (Lund, 2005; table 1). DuRoss and others (2014) excavated trenches across the northern East Bench fault at the Penrose Drive site (figure 1), where an 11-m-high scarp vertically offsets alluvial-fan surfaces and Lake Bonneville lacustrine sediments. Colluvial wedge material in two trenches revealed evidence for five or six earthquakes postdating the Provo-phase shoreline of Lake Bonneville (~14–18 ka) (table 1). While the youngest two earthquakes at Penrose Drive likely correspond with earthquakes interpreted from the Little Cottonwood Canyon and South Fork Dry Creek sites (table 1), the rupture extent of SLCS earthquakes remains uncertain (DuRoss and Hylland, 2015).

Table 1. Correlation of surface-faulting earthquakes on the Salt Lake City segment prior to this study.

Earthquake	Northern East Bench fault	Central Cottonwood fault	
	Penrose Drive (PD) (ka)	Little Cottonwood Cyn. (LCC) (ka)	S. Fork/Dry Creek (SFDC) (ka)
S1	no evidence	1.3 ± 0.04* (Z)	1.3* ± 0.2 (D)
S2	no evidence	2.1 ± 0.3* (Y)	2.2* ± 0.4 (C)
S3	4.0 ± 0.5 (PD1)	4.4 ± 0.5* (X)	3.8* ± 0.6 (B)
S4	5.9 ± 0.7 (PD2)	5.5 ± 0.8* (W)	5.0* ± 0.5 (A)
S5	7.5 ± 0.8 (PD3a)	7.8 ± 0.7* (V)	not exposed
S6	9.7 ± 1.1 (PD3b)	9.5 ± 0.2 (U)	"
S7	10.9 ± 0.2 (PD4)	no evidence	"
S8	12.1 ± 1.6 (PD5)	no evidence	"
S9	16.5 ± 1.9 (PD6)	16.5 ± 2.7* (T)	"

Correlation of surface-faulting earthquakes (S1–S9) on the East Bench and Cottonwood faults after DuRoss and Hylland (2015). Mean and 2σ earthquake times based on OxCal models developed by DuRoss and others (2014) using data from Black and others (1996) and McCalpin (2002). * Indicates earthquake times based on bulk-soil AMRT ages. Text in parentheses (e.g., PD1) refers to site-earthquake names.

At the time of our investigation, important questions remained regarding the timing and rupture extent of surface-faulting earthquakes on the SLCS. For example, some earthquake timing and mean recurrence estimates have large uncertainties because of legacy, apparent mean residence time (AMRT) radiocarbon ages used to constrain the earthquake times. These ages are difficult to interpret because of poorly understood soil fractions and residence times that contribute to the resulting radiocarbon age (Nelson and others, 2006). Further, questions remain regarding the extent of past surface-faulting earthquakes. For example, were recent ruptures limited to the 40-km long SLCS, or have shorter or longer ruptures occurred? Shorter ruptures

could have been limited to one or two of the segment's three separate fault strands, whereas longer ruptures would imply rupture across segment boundaries to the north or south, perhaps as spillover onto the PS. These questions are fundamental to understanding the segmentation of the central WFZ and the moment release of past and future large earthquakes. However, previous paleoseismic data for the SLCS are limited and insufficient to address questions of rupture extent.

Here, we discuss paleoseismic methods and data from the Corner Canyon trench site on the southern Cottonwood fault. Site mapping, trench excavation, and numerical dating methods are described in detail, as well as trench stratigraphy and preliminary data analysis.
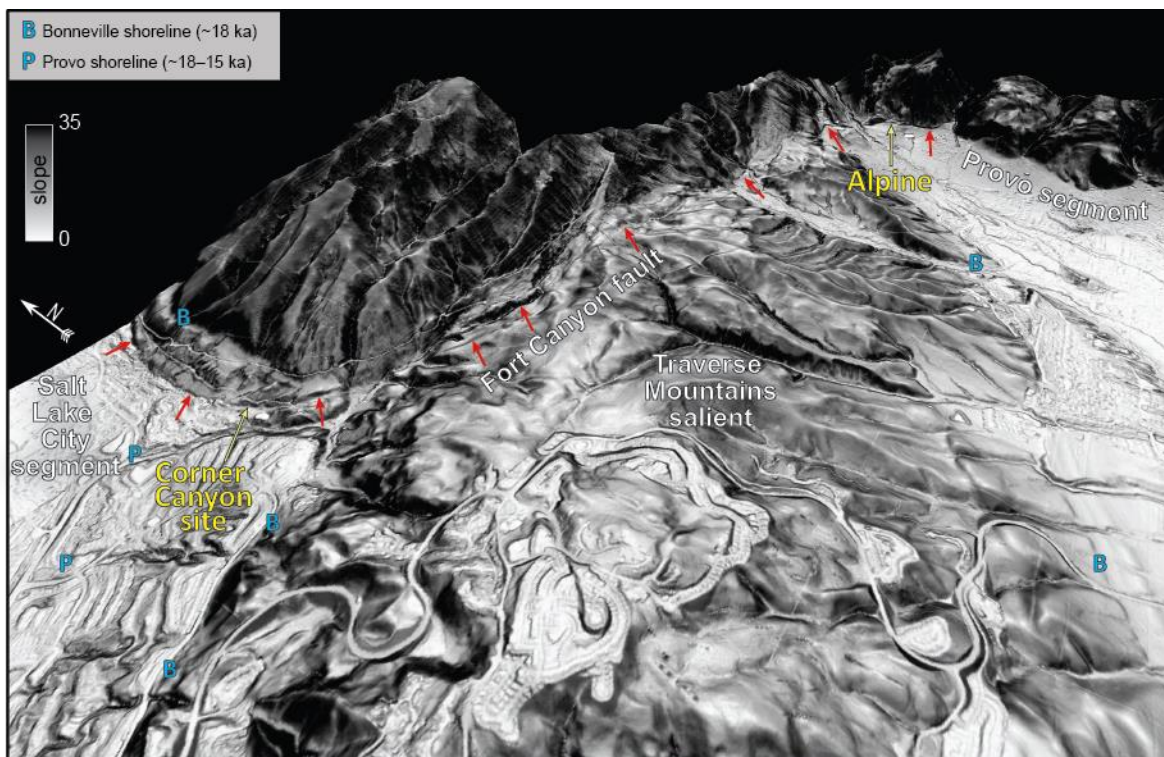
Figure 2. Oblique east view of slope-shade map of the Traverse Mountains salient, showing fault scarps (red arrows) along the southernmost Salt Lake City segment and northernmost Provo segment of the WFZ. Corner Canyon and Alpine (Bennett and others, 2015) trench sites shown in yellow. Bonneville shoreline shown with blue "B", Provo shoreline shown with blue "P." Slope-shade map created from 2013-2014 AGRC lidar data.

CORNER CANYON TRENCH SITE

We excavated a ~40-m long and ~3–4-m deep trench across the Cottonwood fault scarp at the Corner Canyon trench site on the SLCS (figure 2) on June 19, 2014. We selected the site based on geologic mapping by Personius and Scott (1992), discussions of SLCS paleoseismic data by the Utah Quaternary Fault Parameters Working Group (UQFPWG, e.g., Lund, 2005, 2007), interpretation of 1958 (U.S. Department of Agriculture [USDA], Commodity Stabilization Service [CSS], 1958) and 1970s aerial photographs (low-sun-angle; Cluff and others, 1970; included in Bowman and others, 2015), 2006–2011 orthophotography from the

National Agricultural Imagery Program (NAIP) (USDA, 2013; Utah Automated Geographic Reference Center [AGRC], 2013), 2-m and 0.5-m-posting Light Detection and Ranging (lidar) data for Salt Lake Valley (AGRC, 2013), and field reconnaissance.

At the Corner Canyon site a ~9-m-high, west-facing fault scarp on post-Provo-shoreline (younger than ~14 ka) alluvial-fan deposits is continuous (undisturbed) for about 85 m. An approximately 1-m-high antithetic fault scarp at the site forms a roughly 30-m-wide graben (figure 3 and 4). The Corner Canyon site was our preferred site because of (1) the simple SLCS surface-trace geometry in the area, (2) the moderately large height of the scarp (~9 m), (3) minimal evidence for scarp modification based on historical 1950s and 1970s aerial photographs (USDA CSS, 1958; Cluff and others, 1970), (4) the location of the site on the southernmost SLCS that would allow us to evaluate the potential for coseismic rupture of the SLCS and PS, and (5) the opportunity to fill an important gap in paleoseismic data on this densely populated part of the WFZ.

Here we discuss three project tasks as outlined in our proposal. The tasks are: (1) geologic mapping, (2) trench excavation, and (3) data analysis.
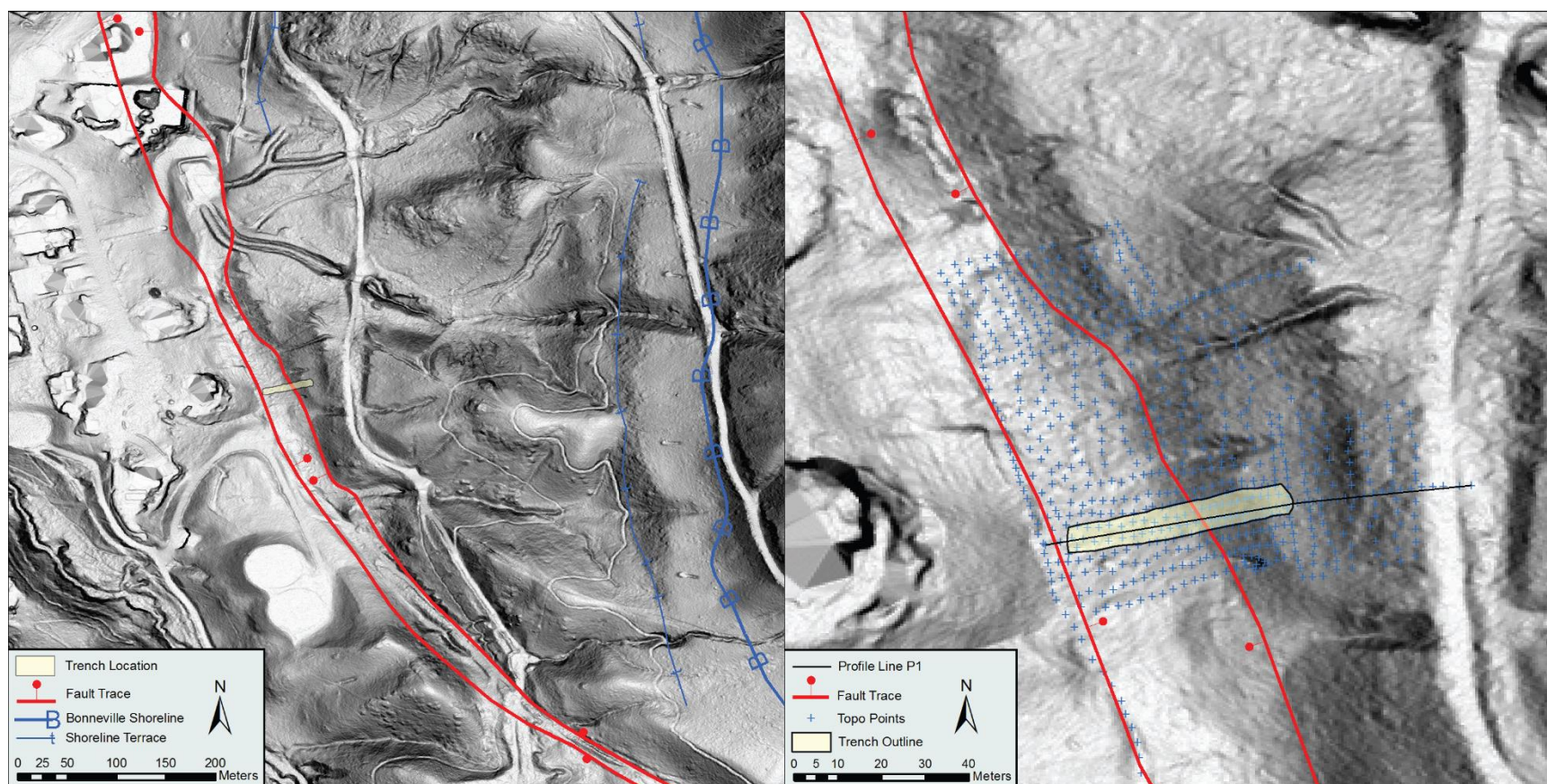
Figure 3. *LEFT: Slope-shade map showing trench location and geologic features. RIGHT: Slope-shade map showing trench location, topographic survey points, and trench profile line P1. Holocene fault traces are shown in red, Bonneville shoreline terraces shown in blue, bar and ball on downthrown side of fault. Slope-shade basemap from 2013-2014 0.5-m AGRC lidar.*
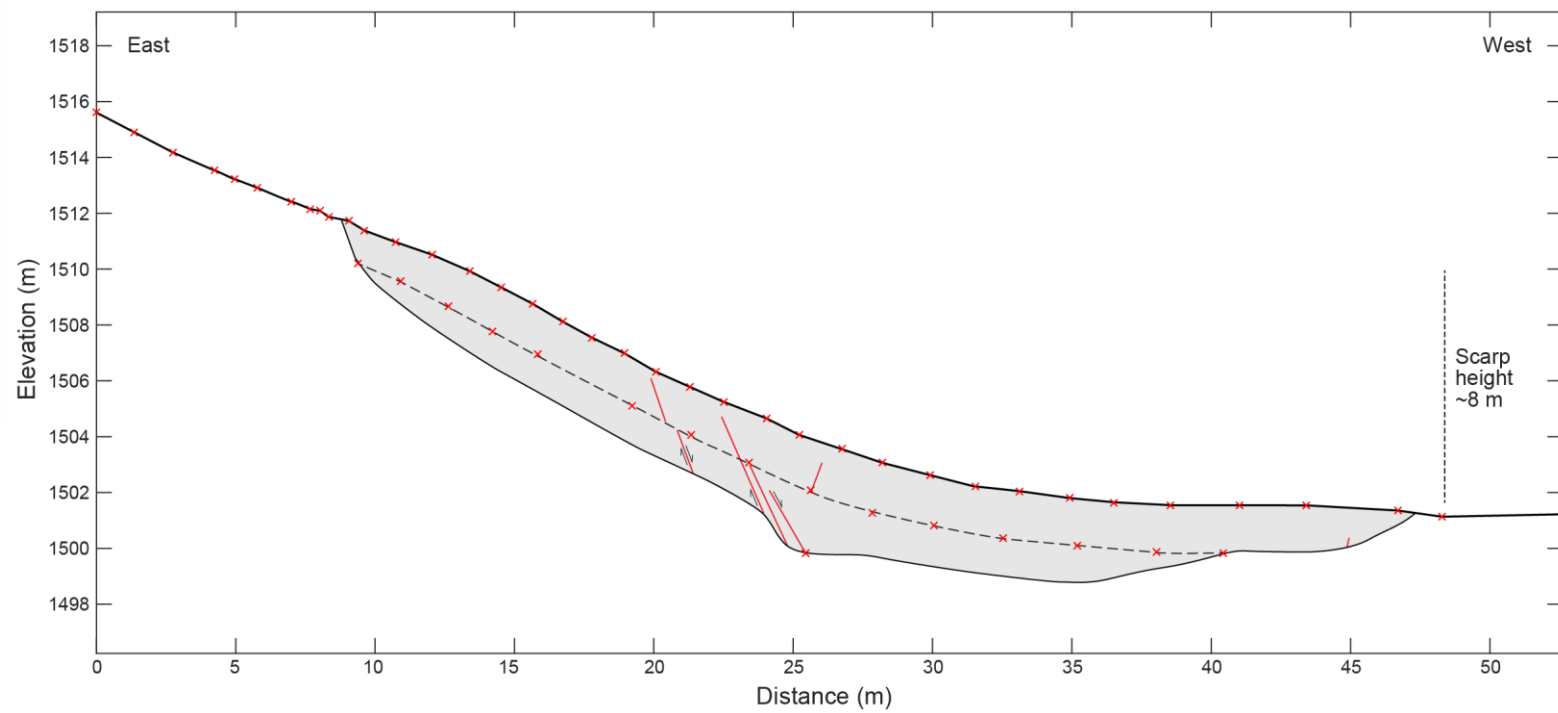
Figure 4. *Scarp profile P1 measured across the Corner Canyon site. Profile points (X's) measured using survey-grade GPS instrumentation. Bench location shown as dashed line. Approximate trench excavation shown as shaded region; fault locations shown in red.*

Task 1 - Geologic Mapping

We completed detailed surficial geologic mapping in the vicinity of the trench site. Following geologic interpretation of 1958 (USDA CSS, 1958), 1970s (low-sun-angle; Cluff and others., 1970; included in Bowman and others, 2015), and 2006–2011 (USDA, 2013) aerial photographs and 2.0-m and 0.5-m-posting lidar derivative maps (e.g., hillshade and slope-shade maps), the locations of key geologic contacts and geomorphic features (e.g., shorelines and fault scarps) were mapped at about 1:10,000 scale (figure 3). We also used survey-grade GPS instrumentation to measure long (~50–100 m) profiles across the fault zone at the site (figures 3 and 4). These profiles will help constrain vertical offsets and slip rates.

Task 2 - Trench Excavation

This task included (1) excavating, cleaning, constructing photomosaics, and interpreting/logging trench exposures (figure 5 shows trench excavation); (2) describing stratigraphic and pedologic units; and (3) collecting samples for radiocarbon and OSL dating.

Figure 5. *Photo of the Corner Canyon trench. Fault zone shown in red with hanging wall (HW) and footwall (FW) annotated. Arrow shows direction of movement on fault. Photo direction is SW. Photo taken on June 22, 2014.*

Methods

Numerical Dating: We sampled bulk soil A horizon sediment and discrete charcoal for radiocarbon (^{14}C) dating to estimate the ages of buried sediments. We collected 35 bulk-soil and macro-charcoal samples, and selected 20 for separation, identification, and ^{14}C dating (appendix B). To increase the likelihood of dating locally derived charcoal, rather than non-local (detrital) charcoal, the bulk soil samples were sent to PaleoResearch Institute in Golden, Colorado for charcoal separation and identification. For discussions of common sources of uncertainty in radiocarbon dating and paleoseismic studies, see Nelson and others (2006) and DuRoss and others (2011).

We submitted the charcoal samples to the National Ocean Sciences Accelerator Mass Spectrometry (NOSAMS) facility of the Woods Hole Oceanographic Institution in Woods Hole, Massachusetts, for accelerator mass spectrometry (AMS) ^{14}C dating. We report the radiocarbon ages as the mean and two-sigma (2σ) uncertainty rounded to the nearest century in thousands of calendar years before 1950 (ka) using the Reimer and others (2009) terrestrial calibration curve applied in OxCal (Bronk Ramsey, 1995, 2001).

We used optically stimulated luminescence (OSL) dating to estimate burial ages of reworked Lake Bonneville and colluvial wedge sediments. We collected 15 OSL samples for dating (appendix C). Our OSL samples were processed at the U.S. Geological Survey Luminescence Dating Laboratory in Denver, Colorado. For more detail on OSL sampling methods, see Gray and others (2015).

Photomosaics: To map the trench-wall exposures, we constructed a 1-meter square grid using a total station instrument (Trimble TTS 500) to project points to an average, vertical plane parallel to the trench walls. We then took approximately 600 photographs of each trench wall, and created photomosaics using the structure-from-motion (SFM) method with Agisoft Photoscan Professional (version 1.0.4) software. For more detail on the SFM method of creating photomosaics, see Reitman and others (2015).

Completed mosaics were printed in 11-by-17 inch sections, corresponding to approximately 4-5 meters horizontal by 3-4 meters vertical sections of the trench wall, for ease of logging. Field logs were digitized using ArcGIS (version 10.2) software and layered portable document format (PDF) files for each trench wall were created, allowing users to toggle individual trench data layers on/off in the PDF.

Trench Stratigraphy

We exposed four distinct sedimentary packages: (1) reworked lacustrine sediments (units 1 and 2), (2) scarp-derived colluvial wedge deposits (units C1 to C7), and (3) alluvial-fan deposits (units 3 and 4). Buried soil A horizons (e.g., soil C6A) are developed within these sedimentary packages, but are best developed and expressed in the colluvial wedge and alluvial-fan deposits. For complete trench stratigraphy and structure, see plates 1 and 2.

Unit 1 consists of colluviated Lake Bonneville lacustrine sand and gravel in the footwall of the fault. Four subunits (units 1a, 1b, 1c, and 1d) are defined on the basis of subtle color and textural changes and the presence of incipient ~0.2-m-thick soil A horizons, and have sub-horizontal to gently west-dipping contacts. We interpret the sediments as reworked (colluviated) rather than related to primary lacustrine deposition because of the overall lack of continuous, fine- to medium-scale bedding throughout the unit. Unit 1 was likely deposited as a result of local erosion and sheet wash which may have occurred concurrently with pedogenic soil development and disturbance (e.g., soil mixing). The origin of sand and gravel in unit 1 is likely nearshore Bonneville sediments that are abundant on slopes above the trench site. The abundance of gullies and levees in the Bonneville sand and gravel demonstrate that these sediments are easily eroded and mobilized. We consider an alluvial origin for unit 1 unlikely because of the well-sorted, but unstratified nature of the unit, which contrasts with the continuous, fine bedding present in alluvial-fan deposits in the hanging wall (units 3 and 4). A total of five ^{14}C and OSL ages for unit 1 are <7 ka, which is considerably younger than the ~18-ka time of the Lake Bonneville highstand, and thus consistent with a reworked origin. A 5-kyr (~2–7-ka) spread in the ages for unit 1 is problematic, but may be related to widespread mixing of soil and sediment throughout the history of deposition. We have the most confidence in the 6.7-ka age for unit 1c, which is consistent with the dominantly ~5–6-ka ^{14}C and OSL ages for unit 2 in the hanging wall.

Unit 2 consists of colluviated lacustrine sand and gravel in the fault hanging wall that is similar in color and texture to unit 1. Unit 2 is locally massive to poorly stratified, but includes a more prominent, ~0.1–0.3-m thick buried soil A horizon (unit 2bA) than those exposed within unit 1. We interpret a similar origin for unit 2 as that for unit 1 on account of the well sorted, but poorly stratified nature of the sediments, and rule out a colluvial wedge origin because of the lack of dispersed soil organics and its generally tabular unit shape. Excluding sample L3 from unit 2c due to stratigraphic inconsistencies, a total of four ^{14}C and OSL ages for unit 2 range from 3.5 to 5.9 ka. We have greater confidence in the older age range as three ages are between 5 and 6 ka (R16, R25, and L5), and a charcoal sample from the base of the oldest colluvial wedge (R19 from unit C6), which likely contained soil sediment eroded from unit 2bA, yielded a similar age of 6.1 ka. Further, additional ages for unit C6, which directly overlies unit 2, indicate a time of deposition at ~3–4 ka, consistent with the 5–6-ka age for unit 2.

Units C6 to C1 (from oldest to youngest) are scarp-derived colluvial wedges formed in response to surface-faulting earthquakes. The units generally consist of massive sand and gravel derived from unit 1 and soil organics that are either dispersed throughout the wedges (C6–C4) or concentrated in A horizons near the tops of the wedges (C3–C1). We mapped an additional small colluvial wedge unit C7 in the footwall on the south wall only. Here, we discuss the lower (units C6–C4) and upper (units C3–C1) wedge units separately.

The lower wedges are characterized by dispersed soil organics and subtle differences in color and texture that, together with fault terminations, form the basis for unit contacts. We observed several upward terminations of minor-displacement normal faults at the bases of units C6 and C4. Other evidence for separate units includes grading in C6 and C5 (both have coarser basal sediments), which may indicate the grading of clasts on a slope and/or concentrated soil organics and silt at the tops of these units (units C6A and C5A). Further, unit C4 has a darker

color than C6 and C5, indicating that unit C4 may have had more time for soil development. Units C6 to C4 are weakly wedge shaped (the wedge geometry is most apparent in the north-wall exposure for C6 and C5) and have maximum thicknesses of 60–80 cm (table 2). A total of 12 ^{14}C and OSL ages provide limits on the timing of C6 to C4 deposition. Excluding possibly recycled charcoal derived from the bases of C6 and C5 (R19 and R22), C6 was deposited at ~3–4 ka (samples L4, L7, and R21) and C5 at ~2.3 ka (R3 and L8). Deposition of unit C4 occurred between ~0.9 and 1.5 ka, based on three samples (R7, R8, and L9). We exclude additional samples for C4 that indicate a younger age (~0.5 ka; R10 and R11) as they are stratigraphically inconsistent with the ages for C3 to C1.

The upper wedges have distinct soil A horizons, back-rotated contacts (C2 and C3), and fault terminations and eroded free faces that help differentiate three separate units (oldest to youngest, C3 to C1). Soil A horizons within the wedges include C3A, C2A, and C1A, which are about 0.1–0.3-m thick. We observed upward fault terminations at the bases of C3 and C1, but not C2. Units C3 to C1 are clearly wedged shaped and have maximum thicknesses ranging from 50 to 85 cm (table 2). Unit C2 is only 50 cm thick, but we interpret this as a separate unit on account of (1) back rotation of the prominent soil developed below C2 in uppermost C3, (2) clear evidence for faulting within unit C2, (3) slope fabric and soil development present within C2, and (4) similar relations expressed in both trench walls. Unit C1, the youngest colluvial wedge, is not faulted, and includes small slope-parallel lenses of sand and gravel that locally bury both C2 and C3. A total of 15 ^{14}C and OSL ages provide limits on the timing of C3 to C1 deposition. Excluding four ages (R9, R12a, R29a, and L11) that are clearly out of stratigraphic order, C3 to C1 were deposited between ~1.0 and 0.4 ka. Unit C3 was deposited at about 1.0 ka (L10), but may be as young as ~0.5 ka (R12b and R12c). C2 deposition likely occurred between ~0.9 ka (R28) and 0.5–0.6 ka (L12 and R29b). C1 postdates samples dated to ~0.4 ka (R15 and R17), but could be as old as 0.7 ka (R32).

Units 3 and 4 consist of well-stratified sand and gravel related to alluvial-fan sedimentation on the hanging wall of the fault within the fault graben. These units reach a maximum thickness of about 1 m and overlie colluvial wedge units C6 to C1. The fan sediments form two distinct packages separated by a thin, organic-rich layer within the uppermost part of unit 3. The lower package (unit 3) postdates C5, and may postdate or be contemporaneous with C4. The upper package (unit 4) postdates C4, and may postdate or be contemporaneous with C3 and C1. Maximum ages for units 3 and 4 are provided by OSL samples L2 and L1 at 2.1 ka and 0.5 ka, respectively.

Trench Structure

The Wasatch fault zone is expressed as a steeply west-dipping normal shear zone accompanied by subparallel synthetic and east-dipping antithetic faults. In the lower wall, the fault forms about a 0.2 to 0.7-m thick zone of sheared sediment that dips 55° to 67° W. In the upper walls, a single fault trace dips 67° W. These faults and associated free-faces juxtapose unit 1 against colluvial wedge units C6 to C1 (figure 6). Numerous synthetic and antithetic faults are steeply dipping to vertical and form an approximately 20-m-wide graben. A lone synthetic fault in the footwall, about 2-m east of the fault adjacent to units C6–C1, dips steeply west with <1-m displacement (mapped in the south wall exposure, plate 1).
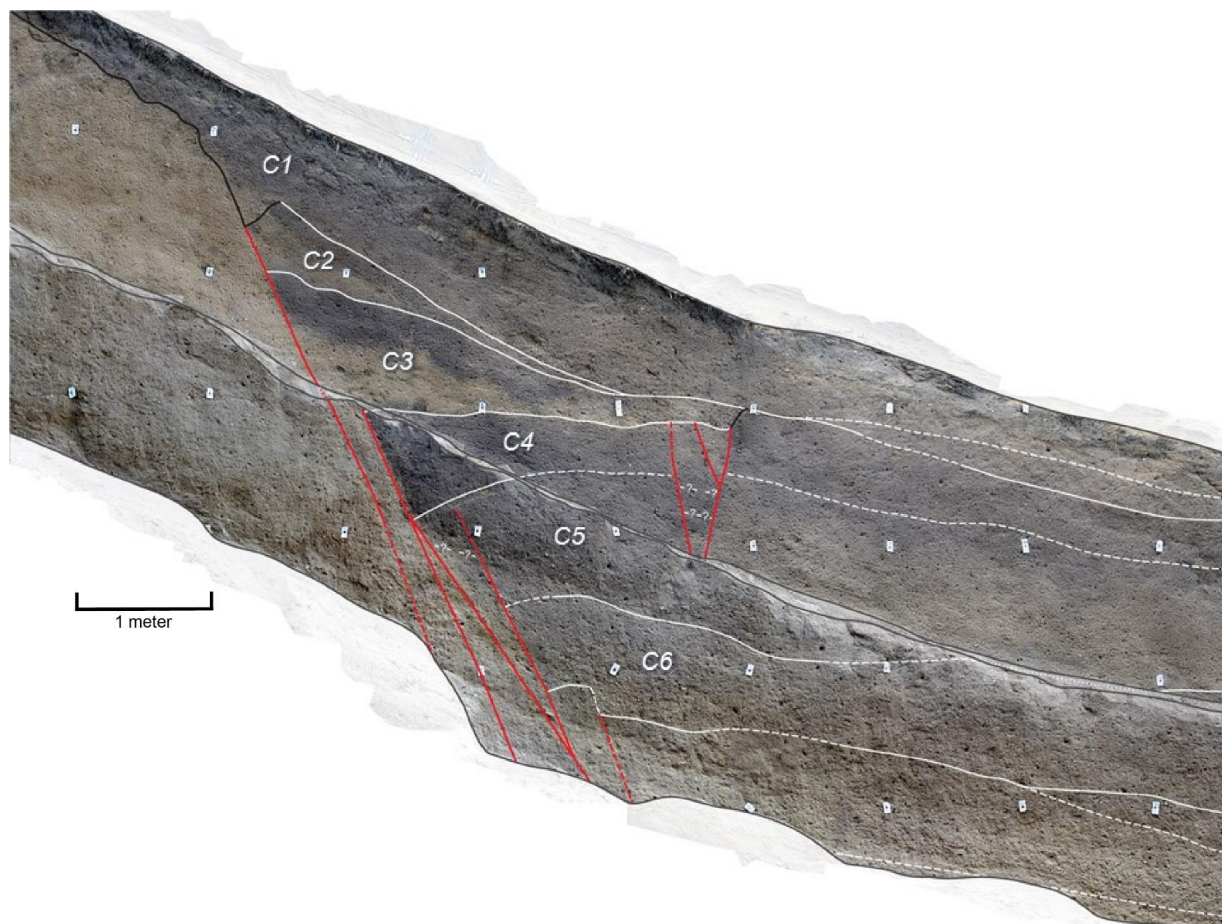
Figure 6. Photomosaic showing the fault zone in the south wall of the trench at the Corner Canyon site. Colluvial wedges annotated as C1, C2, etc. Stratigraphic contacts shown in white, faults shown in red. Contacts dashed where approximate.

The total displacement across the Corner Canyon trench is poorly constrained because of the incomplete exposure of the entire graben, due to a high pressure Questar natural gas line running along the western extent of the trench. As a result, considerable uncertainty exists in how to project the oldest faulted unit in the hanging wall (unit 2) toward the main fault zone. Further, contacts between subunits 1a, 1b, and 1c are sub-horizontal to gently west dipping, and thus, shallower than the ground surface slope above the scarp crest. Using projections of the upper (top of unit 1) and lower (top of unit 2bA and 2c) surfaces yields a total vertical displacement of 4.6 to 7.1 m (midpoint of 5.9 m). We consider this displacement measurement to be poorly characterized because of the limited footwall exposure and uncertainty in whether additional antithetic faults exist west of the westernmost graben-bounding fault. However, our measurement is consistent with the vertical-offset measurement of 6.1 m made by Personius and Scott (1992) <0.1 km north of the site. Comparably, colluvial wedge units C6 to C1 have maximum thicknesses ranging from 0.5 to 0.9 m (table 2), indicating a minimum of 4.2 m of vertical displacement at the site.

Table 2. *Evidence for surface-faulting earthquakes at the Corner Canyon site.*

Unit[1]	Geometry	Basal contact	Texture	Soil	Fault terminations[2]	Fault rotation[3]	Notes
C1	Wedge shaped with heel; 80 cm maximum thickness	Clear lower contact with soil C2A	Massive to weakly bedded with slope fabric	Dispersed organics; modern A horizon (C1A) at top	One	Not faulted	Buried free face; similar in both walls
C2	Wedge shaped; 50 cm maximum thickness	Clear lower contact with soil C3A	Massive to weakly bedded with slope fabric	Minor dispersed organics; A horizon (C2A) at top (~10 cm)	None	Back rotation of soil below C2	Base obscured (burrowed?) in north wall
C3	Wedge shaped; 85 cm maximum thickness	Very clear lower contact with soil C4A	Massive to weakly bedded with slope fabric	Almost no organics in wedge; A horizon (C3A) at top (25-35 cm)	Possible	Clearly back rotated; angular unconformity at base	Similar in both walls
C4	Weakly wedge shaped; 60 cm maximum thickness	Diffuse lower contact with C5	Massive	Dispersed organics; A horizon near top (C4A); unknown thickness	Multiple	Back rotation adjacent to fault zone	Similar in both walls, but east edge faulted by subsidiary fault in north wall
C5	Weakly wedge shaped; 70-80 cm maximum thickness	Clear to diffuse lower contact with C6A	Massive, but graded (coarser basal sediments)	Dispersed organics; no apparent soil formation	Possible	No rotation apparent; structural unconformity where younger faulting steps east	Wedge geometry in north wall; includes possible graben-fill sediments
C6	Weakly wedge shaped to tabular; 70 cm maximum thickness	Diffuse lower contact with buried A	Massive, but graded (coarser basal sediments)	Dispersed organics; weak A (C6A) in upper part (~20 cm)	Possible	No rotation apparent; structural unconformity where younger faulting steps east	Wedge geometry in north wall; includes possible graben-fill sediments

[1] Unit corresponds to plate 1.
[2] Fault terminations are upward terminations below base of wedge, or outside of the fault zone, at a contact that is consistent with the stratigraphic position of the base of the wedge.
[3] Back rotation is rotation of soil, sediment, or surface on hanging wall down toward fault zone.

Task 3 - Data Analysis

Analysis of colluvial wedge stratigraphy, fault terminations, and weakly to well-developed soil A horizons shows evidence for potentially six surface-faulting earthquakes at the Corner Canyon trench site. Colluvial wedge thicknesses of ~0.5–0.9 m indicate a possibility of ~1-2 m of vertical offset per earthquake. Preliminary data of the 20 ^{14}C and 11 OSL samples submitted for processing shows that potentially six earthquakes (CC1–CC6) occurred at the site since ~5 ka. The timing of CC1–CC6 presented here are preliminary. We plan to further analyze these data by constructing time-stratigraphic OxCal models (Bronk Ramsey 1995, 2001) for the site.

Three to four SLCS earthquakes previously identified at the Penrose Drive (PD), Little Cottonwood Canyon (LCC) and South Fork Dry Creek (SFDC) sites (DuRoss and Hylland, 2015) likely ruptured the Corner Canyon site (table 1). The oldest earthquake at the Corner Canyon site, CC6, likely occurred at ~4–5 ka, which could correspond with SLCS earthquake S4 at ~5.0–5.9 ka. Earthquake CC5 ruptured the site at approximately 3–4 ka, corresponding to SLCS earthquake S3 at ~3.8–4.0 ka. Earthquake CC4 likely occurred at ~2 ka, corresponding to SLCS earthquake S2 at ~2.1–2.2 ka. Finally, earthquake CC3 likely occurred at ~1 ka, similar to SLCS earthquake S1 at ~1.3 ka. CC2 and CC1 are younger than 1 ka, and thus postdate the youngest earthquakes previously identified on the SLCS (S1 and S2 at the LCC and SFDC trench sites) (table 1).

Two Corner Canyon earthquakes occurred after ~1.0 ka. As these earthquakes have not been identified elsewhere on the SLCS, it is possible that one or both may correlate with previously identified earthquakes on the PS (e.g., DuRoss and others, 2016). Further analysis and OxCal modeling of the Corner Canyon data, analysis of previous data for the SLCS and PS, and comparison of our data to results from the Alpine trench site (Bennett and others, 2015) will facilitate a more in-depth analysis of timing, length, and frequency of past SLCS earthquake ruptures.

Using these preliminary data, we calculate a mean recurrence interval of ~0.9 kyr for the Corner Canyon site, in contrast to a mean recurrence of ~1.3 kyr for previously identified earthquakes on the SLCS (DuRoss and Hylland, 2015). The shorter mean recurrence may be due to PS spillover rupturing the Corner Canyon site but not other sites farther north on the SLCS.

CONCLUSIONS

Preliminary data from the Corner Canyon trench site suggest four of the six earthquakes identified at Corner Canyon have rupture chronologies that are similar to previously documented earthquakes on the SLCS. Preliminary data also indicate two younger (post ~1 ka) earthquakes at the site that postdate any previously identified SLCS earthquakes. These results suggest that the Corner Canyon site has experienced more earthquake ruptures than the central part of the SLCS, and thus may record spillover events from the PS. Continued analysis of the Corner Canyon paleoseismic data and a comparison of these data with previous earthquake records for the SLCS and PS will help resolve the timing and rupture parameters (partial or multi-segment rupture) of

past SLCS earthquakes. Additionally, the paleoseismic data obtained in this study will be used to update the UGS *Utah Quaternary Fault and Fold Database*, the USGS *Quaternary Fault and Fold Database of the United States*, and the USGS National Seismic Hazard Maps.

REFERENCES

Bennett, S.E.K., DuRoss, C.B., Gold, R.D., Briggs, R.W., Personius, S.F., Reitman, N.G., Hiscock, A.I., DeVore, J.D., Gray, H.J., and Mahan, S.A., 2015, History of six surface-faulting Holocene earthquakes at the Alpine trench site, northern Provo segment, Wasatch fault zone, Utah: Seismological Research Letters, v. 86, no. 2B, p. 671.

Birkeland, P.W., Machette, M.N., and Haller, K.M., 1991, Soils as a tool for applied Quaternary geology: Utah Geological and Mineral Survey Miscellaneous Publication 91-3, 63 p.

Black, B.D., Lund, W.R., Schwartz, D.P., Gill, H.E., and Mayes, B.H., 1996, Paleoseismic investigation on the Salt Lake City segment of the Wasatch fault zone at the South Fork Dry Creek and Dry Gulch sites, Salt Lake County, Utah—Paleoseismology of Utah, Volume 7: Utah Geological Survey Special Study 92, 22 p., 1 plate.

Bowman, S.D., Hiscock, A.I., and Unger, C.D., 2015, Compilation of 1970s Woodward-Lundgren & Associates Wasatch fault investigation reports and low-sun-angle aerial photography, Wasatch Front and Cache Valley, Utah and Idaho – Paleoseismology of Utah, Volume 26: Utah Geological Survey Open-File Report 632, 8 p., 6 plates, 9 DVD set.

Bronk Ramsey, C., 1995, Radiocarbon calibration and analysis of stratigraphy—the OxCal program: Radiocarbon, v. 37, no. 2, p. 425–430.

Bronk Ramsey, C., 2001, Development of the radiocarbon program OxCal: Radiocarbon, v. 43, no. 2a, p. 355–363.

Bruhn, R., Gibler, P., Houghton, W., and Parry, W., 1992, Structure of the Salt Lake segment, Wasatch normal fault zone—implications for rupture propagation during normal faulting, *in* Gori, P.L., and Hays, W.W., editors, Assessment of regional earthquake hazards and risk along the Wasatch Front, Utah: U.S. Geological Survey Professional Paper 1500-A-J, p. H1–H25.

Cluff, L.S., Brogan, G.E., and Glass, C.E., 1970, Wasatch fault, northern portion—earthquake fault investigation and evaluation, a guide to land-use planning: Oakland, California, Woodward-Clyde and Associates, unpublished consultant report for the Utah Geological and Mineralogical Survey, variously paginated, compiled in Bowman and others, 2015.

DuRoss, C.B., Bennett, S.E.K., Hiscock, A.I., Personius, S.F., Gold, R.D., Briggs, R.W., Reitman, N.G., Devore, J.D., and Mahan, S.A., 2015, Multiple Holocene surface-faulting earthquakes at the Corner Canyon trench site on the Salt Lake City segment of the Wasatch fault zone, Utah: Seismological Research Letters, v. 86, no. 2B, pg. 671.

DuRoss, C.B. and Hylland, M.D, 2015, Synchronous ruptures along a major graben-forming fault system—Wasatch and West Valley fault zones, Utah: Bulletin of the Seismological Society of America, v. 105, no. 1, p. 14-37, doi:10.1785/0120140064.

DuRoss, C.B., Hylland, M.D., McDonald, G.M., Crone, A.J., Personius, S.F., Gold, R.D., Mahan, S.A., 2014, Holocene and latest Pleistocene paleoseismology of the Salt Lake City segment of the Wasatch fault zone, Utah, at the Penrose drive trench site, *in* DuRoss, C.B., and Hylland, M.D., Evaluating surface faulting chronologies of graben-bounding faults in Salt Lake Valley, Utah—new paleoseismic data from the Salt Lake City segment of the Wasatch fault zone and the West Valley fault zone – Paleoseismology of Utah, Volume 24: Utah Geological Survey Special Study 149, 39 p., 1 plate, 6 appendices.

DuRoss, C.B., Personius, S.F., Crone, A.J., Olig, S.S., Hylland, M.D., Lund, W.R., and Schwartz, D.P., 2016, Fault segmentation: New concepts from the Wasatch fault zone, Utah, USA: Journal of Geophysical Research—Solid Earth, v. 121, 27 p., doi:10.10002/2015JB012519.

DuRoss, C.B., Personius, S.F., Crone, A.J., Olig, S.S., and Lund, W.R., 2011, Integration of paleoseismic data from multiple sites to develop an objective earthquake chronology–Application to the Weber segment of the Wasatch fault zone: Bulletin of the Seismological Society of America, v. 101, no. 6, p. 2765-2781.

Gray, H.J., Mahan, S.A., Rittenour, T., and Nelson, M., 2015, Guide to luminescence dating techniques and their applications for paleoseismic research, *in* Lund, W.R., editor, 2015, Proceedings volume, Basin and Range Province Seismic Hazards Summit III (BRPSHSIII): Utah Geological Survey Miscellaneous Publication 15-5, variously paginated.

Lund, W.R., 2005, Consensus preferred recurrence-interval and vertical slip-rate estimates—review of Utah paleoseismic-trenching data by the Utah Quaternary Fault Parameters Working Group: Utah Geological Survey Bulletin 134, 109 p.

Lund, W.R., 2007, Summary—Utah Quaternary Fault Parameters Working Group Annual Meeting—Wednesday, February 28, 2007: Utah Geological Survey unpublished summary of the Utah Quaternary Fault Parameters Working Group, 13 p.

Lund, W.R., 2010, Summary—Third Meeting; Working Group on Utah Earthquake Probabilities—Wednesday & Thursday, December 1 & 2, 2010: Utah Geological Survey unpublished minutes of the Working Group on Utah Earthquake Probabilities, 16 p.

Machette, M.N., Personius, S.F., and Nelson, A.R., 1992, Paleoseismology of the Wasatch fault zone—a summary of recent investigations, interpretations, and conclusions, *in* Gori, P.L., and Hays, W.W., editors, Assessment of regional earthquake hazards and risk along the Wasatch Front, Utah: U.S. Geological Survey Professional Paper 1500-A-J, p. A1–A71 p.

McCalpin, J.P., 2002, Post-Bonneville paleoearthquake chronology of the Salt Lake City segment, Wasatch fault zone, from the 1999 "megatrench" site—Paleoseismology of Utah, Volume 10: Utah Geological Survey Miscellaneous Publication 02-7, 37 p.

Nelson, A.R., Lowe, M., Personius, S., Bradley, L.A., Forman, S.L., Klauk, R., and Garr, J., 2006, Holocene earthquake history of the northern Weber segment of the Wasatch fault zone,

Utah—Paleoseismology of Utah, Volume 13: Utah Geological Survey Miscellaneous Publication 05-8, 39 p., 2 plates.

Personius, S.F., and Scott, W.E., 1992, Surficial geologic map of the Salt Lake City segment and parts of adjacent segments of the Wasatch fault zone, Davis, Salt Lake, and Utah Counties, Utah: U.S. Geological Survey Miscellaneous Investigations Series Map I-2106, scale 1:50,000.

Prescott, J.R., and Hutton, J.T., 1994, Environmental dose rates and radioactive disequilibrium from some Australian luminescence dating sites: Quaternary Science Reviews, v. 14, no. 4, p. 439-448.

Reimer, P.J., Baillie, M.G.L., Bard, E., Bayliss, A., Beck, J.W., Blackwell, P.G., Bronk Ramsey, C., Buck, C.E., Burr, G.S., Edwards, R.L., Friedrich, M., Grootes, P.M., Guilderson, T.P., Hajdas, I., Heaton, T.J., Hogg, A.G., Hughen, K.A., Kaiser, K.F., Kromer, B., McCormac, F.G., Manning, S.W., Reimer, R.W., Richards, D.A., Southon, J.R., Talamo, S., Turney, C.S.M., van der Plicht, J., and Weyhenmeyer, C.E., 2009, IntCal09 and Marine09 radiocarbon age calibration curves, 0–50,000 years cal BP: Radiocarbon, v. 51, no. 4, p. 1111–1150.

Reimer, P., Bard, E., Bayliss, A., Beck, J., Blackwell, P., Bronk Ramsey, C., Buck, C., Cheng, H., Edwards, R., Friedrich, M., Grootes, P., Guilderson, T., Haflidason, H., Hajdas, I., Hatté, C., Heaton, T., Hoffmann, D., Hogg, A., Hughen, K., Kaiser, K., Kromer, B., Manning, S., Niu, M., Reimer, R., Richards, D., Scott, E., Southon, J., Staff, R., Turney, C., & van der Plicht, J., 2013, IntCal13 and Marine13 radiocarbon age calibration curves 0–50,000 years cal BP: Radiocarbon, v. 55, no. 4, p. 1869-1887.

Reitman, N.G., Bennett, S.E.K., Gold, R.D., Briggs, R.W., and DuRoss, C.B., 2015, High-resolution trench photomosaics from image-based modeling—Workflow and error analysis: Bulletin of the Seismological Society of America, v. 105, no. 5, p. 2354-2366.

Schwartz, D.P., and Lund, W.R., 1988, Paleoseismicity and earthquake recurrence at Little Cottonwood Canyon, Wasatch fault zone, Utah, in Machette, M.N., editor, In the footsteps of G.K. Gilbert—Lake Bonneville and neotectonics of the eastern Basin and Range Province: Utah Geological and Mineral Survey Miscellaneous Publication 88-1, p. 82–85.

Scott, W.E., and Shroba, R.R., 1985, Surficial geologic map of an area along the Wasatch fault zone in the Salt Lake Valley, Utah: U.S. Geological Survey Open-File Report 85-448, 18 p., 2 plates, scale 1:24,000.

Swan, F.H., III, Hanson, K.L., Schwartz, D.P., and Black, J.H., 1981, Study of earthquake recurrence intervals on the Wasatch fault at the Little Cottonwood Canyon site, Utah: U.S. Geological Survey Open-File Report 81-450, 30 p.

U.S. Department of Agriculture, Commodity Stabilization Service, 1958, Aerial photography, Project AAL, frames 16V-20–22, dated 5-27-1958, black and white, approximate scale 1:10,000, available at http://geology.utah.gov/databases/imagery/index.php.

U.S. Department of Agriculture, 2013, Aerial Photography Field Office, National Agriculture Imagery Program: Online, http://www.fsa.usda.gov/FSA/apfoapp?area=home&subject=prog&topic=nai, accessed May 2013.

Utah Geological Survey, Utah Quaternary Fault and Fold Database, 2016: Online, http://geology.utah.gov/resources/data-databases/qfaults/

Utah Automated Geographic Reference Center, 2013, Utah GIS Portal: Online, http://agrc.its.state.ut.us/, accessed May 2013.

Working Group on Utah Earthquake Probabilities (WGUEP), 2016, Earthquake probabilities for the Wasatch Front region in Utah, Idaho, and Wyoming: Utah Geological Survey Miscellaneous Publication 16-3, 164 p., 5 appendices.

Appendix A. *Description of stratigraphic units at the Corner Canyon site.*

Unit Genesis[1]	Coordinates (Trench, H, V, [m])	Textural Name[2]	Texture (%)[3]				Clasts (cm)		Plasticity[4]	Density/ Consistency[5]	Cementation	HCL Reaction	Clast Angularity	Bedding	Structure	Sorting	Lower Boundary[6]	Color		Notes
			F	S	G	C/B	Largest	Average										Dry[7]	Moist[7]	
1a,HC	N, 8.8, 9.0	gravely sand with minor silt	5	70	25	0	4	0.5	po	so, sh	none	none	round to angular	massive	none	moderately sorted	n/a	10YR 5/4	10YR 4/4	--
1b, HC	N, 8.7, 9.9	gravely sand with silt	10	70	20	0	3	0.5	ps	ss, sh	none	none	round to angular	massive	none	moderately sorted	g, w	10YR 5/4	10YR 4/4	--
1c, HC	N, 9.0, 10.7	gravely sand with silt	10	70	20	0	5.5	0.5	ps	ss, sh	none	none	round to angular	massive	none	moderately sorted	g, w	10YR 5/4	10YR 4/4	--
1d, HC	N, 1.4, 14.5	gravely sand with silt	10	75	15	0	3.5	0.5	ps	ss, sh	none	none	round to angular	massive	none	moderately sorted	g, i	10YR 5/4	10YR 4/4	Modern soil level on upper ~15 cm
C1, FC	N, 15.3, 8.1	gravely sand with silt	10	80	10	0	3.5	0.5	ps	ss, sh	none	none	round to angular	some slope parallel fabric	none	moderately sorted	g to c	10YR 4/4	10YR 3/4	Youngest colluvial wedge (C1); pebble lag at base
C2, FC	N, 15.4, 7.7	gravely sand with silt	10	75	15	0	4	0.5	ps	ss, sh	none	none	round to angular	massive	none	moderately sorted	c, w	10YR 4/4	10YR 3/4	Colluvial wedge C2; faulted soil at top
C3, FC	N, 16.2, 7.0	gravely sand with silt	5	80	15	0	3	0.5	po	so, sh	none	none	round to angular	debris flow and colluvial facies	none	moderately sorted	c, w	10YR 5/4	10YR 4/4	Colluvial wedge C3; Nice pebble lay at toe
C4, FC	N, 16.5, 6.4	gravely sand with silt	5	85	10	0	3.5	0.5	ps	ss, sh	none	none	round to angular	slight slope fabric	none	moderately sorted	d, i	10YR 4/4	10YR 3/3	Colluvial wedge C4
C5, FC	N, 17.9, 5.4	gravely sand with silt	5	90	5	0	3	0.5	ps	ss, sh	none	none	round to angular	massive	none	moderately sorted	g, i	10YR 4/4	10YR 3/3	Colluvial wedge C5
C6, FC	N, 17.8, 5.0	gravely sand with silt	5	90	5	0	3	0.5	ps	ss, sh	none	none	round to angular	massive	none	moderately sorted	c, i	10YR 5/5	10YR 3/3	Colluvial wedge C6
2a, HC	S, 21.0, 3.2	sand with gravel and silt	5	90	5	0	4	0.5	po	so, so	none	none	round to angular	massive	none	moderately sorted	n/a	10YR 6/4	10YR 5/4	--
2b, HC	N, 18.6, 4.1	sand with gravel and silt	5	90	5	0	3	0.5	po	so, sh	none	none	round to angular	massive	none	moderately sorted	c, w	10YR 6/4	10YR 4/4	pebble lag at base in places
2c, HC	N, 18.7, 4.5	sand with gravel and silt	5	90	5	0	7	0.5	ps	ss, sh	none	none	round to angular	massive	none	moderately sorted	g, w	10YR 5/4	10YR 4/4	--
3, S	N, 32.6, 4.0	sand with gravel and silt	5	90	5	0	3.5	0.5	po	so, sh	none	none	round to angular	thinly bedded stream deposits	broadly lenticular	moderately sorted	a, s	10YR 5/4	10YR 3/4	--
4, S	N, 33.0, 4.3	sand with gravel and silt	5	90	5	0	7.5	0.5	po	so, sh	none	none	round to angular	thinly bedded stream deposits	broad lenses	moderately sorted	a, s	10YR 5/4	10YR 4/4	burrows, roots near top

[1] Genesis: **S** - stream, **DF** - debris flow, **L** - lacustrine, **C** - colluvium, **F** – fill, **HC** – hillslope colluvium, **FC** – fault colluvium.

[2] Texture name approximated using the Unified Soil Classification System (density/consistency after Birkeland and others [1991]). Textural information may not be representative of entire unit due to vertical and horizontal heterogeneity in units.

[3] Percentages of clast-size fractions (based on area) are field estimates. **F** - fines (silt and clay), **S** - sand, **G** - gravel, **C/B** - cobbles and boulders. We used a U.S. Standard #10 (2mm) sieve to separate matrix (clay, silt, and sand) from gravel.

[4] Plasticity: **po** - nonplastic, **ps** - slightly plastic, **p** - plastic, **vp** - very plastic.

[5] Wet Density/Consistency: **so** - nonsticky, **ss** - slightly sticky, **s** - sticky, **vs** - very sticky. Dry Density/Consistency: **lo** - loose, **so** - soft, **sh** - slightly hard, **h** - hard, **vh** - very hard, **eh** - extremely hard.

[6] Lower Boundary modified from Birkeland and others (1991). Distinctness: **a** - abrupt (1mm-2.5cm), **c** - clear (2.5-6cm), **g** - gradual (6-12.5cm), **d** - diffuse (>12.5cm). Topography: **s** - smooth, **w** - wavy, **i** - irregular, **ne** - base of unit not exposed.

[7] Munsell color of matrix (year 2000 - revised version).

Appendix B. Radiocarbon ages for the Corner Canyon site.

Sample No.	NOSAMS[1] Accession No.	Unit[2]	Sample Description[3]	Sample wt. (mg)	Lab Age (^{14}C yr B.P.) - mean, $\pm 1\sigma$[4]		δ^{13}C (if measured)	Calibrated age (cal yr B.P.) - 95% range[5]		Calibrated age (cal yr B.P.) - mean, $\pm 1\sigma$[6]		Calibrated age (thous. of cal yr B.P.) - mean, $\pm 2\sigma$[7]	
CC-R3	OS-117244	C5	Charred Juniper berry	7.8	2290	15	-25.8	2350	2310	2327	25	2.3	0.1
CC-R7	OS-117245	C4	Charred Juniper berry	6.0	980	15	-25.87	934	802	895	40	0.9	0.1
CC-R8	OS-117246	C4	Charred Juniper berry	6.4	1360	15	-25.09	1304	1277	1290	6	1.3	0.01
CC-R9	OS-117247	C3	Charred Juniper berry	1.5	2440	15	*Not meas.*	2687	2361	2509	104	2.5	0.2
CC-R10	OS-117248	C4	Artemisia charcoal	2.7	350	15	-27.51	481	318	398	52	0.4	0.1
CC-R11	OS-117249	C4	Charred Juniper berry	4.9	470	15	-25.61	528	503	515	6	0.5	0.01
CC-R12a	OS-117250	C3	Unidentified seeds (charred)	9.0	2270	15	-25.79	2345	2184	2296	50	2.3	0.1
CC-R12b	OS-117251	C3	Rosaceae charcoal	4.9	395	15	-24.93	506	336	472	40	0.5	0.1
CC-R12c	OS-120983	C3	Unidentified hardwood charcoal	2.7	470	15	-25.46	528	503	515	6	0.5	0.01
CC-R15	OS-117252	C1	Charred Juniper berry	6.3	315	15	-25.52	451	306	382	39	0.4	0.1
CC-R16	OS-117253	2	Charred Juniper berry	1.9	4520	20	*Not meas.*	5303	5053	5164	75	5.2	0.2
CC-R17	OS-117254	C1	Charred Juniper berry	0.9	380	15	*Not meas.*	501	332	445	55	0.4	0.1
CC-R19	OS-117255	C6	Charred Juniper berry	2.6	5340	20	-25.5	6208	6003	6110	60	6.1	0.1
CC-R21	OS-117080	C6	Charred Juniper berry	7.2	3140	25	-25.76	3444	3257	3361	40	3.4	0.1
CC-R22	OS-117081	C5	Charred Juniper berry	7.5	3220	25	-25.73	3544	3380	3433	32	3.4	0.1
CC-R25	OS-117082	2	Charred Juniper berry	2.5	4700	40	-24.94	5581	5319	5431	78	5.4	0.2
CC-R26a	OS-116960	C3	Charred Juniper berry	10.5	325	20	-26.09	460	308	385	43	0.4	0.1
CC-R26b	OS-121089	C3	Rosaceae charcoal	1.2	380	20	-24.5	504	327	437	58	0.4	0.1
CC-R28	OS-117492	C2	Charred Juniper berry	4.0	940	20	-25.58	920	796	854	37	0.9	0.1
CC-R29a	OS-117493	C2	Charred Juniper berry	3.5	2110	20	-26.46	2145	2005	2081	38	2.1	0.1
CC-R29b	OS-120883	C2	Unidentified hardwood charcoal	1.3	660	20	-25.01	670	561	615	39	0.6	0.1
CC-R30	OS-117494	1	Charred Juniper berry	5.0	5870	35	-26.42	6785	6569	6692	41	6.7	0.1
CC-R32	OS-117495	C1	Charred Juniper berry	3.1	740	20	-26.61	699	661	679	9	0.7	0.02
CC-R33	OS-117496	1	Charred Juniper berry	0.7	3680	30	*Not meas.*	4139	3914	4019	51	4.0	0.1

[1] National Ocean Sciences Accelerator Mass Spectrometry Facility, Woods Hole Oceanographic Institution (Woods Hole, Massachusetts).

[2] Units correspond to plates 1 and 2.

[3] Charcoal separation and identification by Paleo Research Institute (Golden, Colorado).

[4] Laboratory-reported radiocarbon age with one standard deviation (1σ) uncertainty. B.P. is before present (AD 1950).

[5] Calendar-calibrated age, 5th – 95th percentile range.

[6] Mean calendar-calibrated age and 1σ uncertainty, determined using OxCal calibration software (v. 4.2; Bronk Ramsey, 1995, 2001) and the IntCal13 atmospheric data set (Reimer and others, 2013).

[7] Mean calendar-calibrated age rounded to nearest century, in thousands of years B.P.; 2σ uncertainty shown.

Appendix C. Optically stimulated luminescence ages for the Corner Canyon site.

Sample No.[1]	Unit sampled[2]	Water content[3]	K (%)[4]	U (ppm)[4]	Th (ppm)[4]	Cosmic dose (Gy/ka)[5]	Total Dose Rate (Gy/ka)	Equivalent Dose (Gy)	N[6]	Scatter[7]	Age (years before 2014) – mean ± 1σ[8]	Age (ka) – mean ± 2σ[9]
CC-L1	3	5 (28)	3.05 ± 0.05	2.34 ± 0.23	11.6 ± 0.5	0.25 ± 0.02	4.50 ± 0.12	2.05 ± 0.22	7 (20)	112%	460 ± 70	0.5 ± 0.1
CC-L2	C5	3 (24)	3.01 ± 0.06	2.09 ± 0.23	12.5 ± 0.54	0.24 ± 0.02	4.50 ± 0.13	9.31 ± 0.33	10 (24)	32%	2,070 ± 90	2.1 ± 0.2
CC-L3	2c	4 (20)	3.41 ± 0.07	2.91 ± 0.23	15.3 ± 0.48	0.20 ± 0.02	5.28 ± 0.11	4.28 ± 0.25	6 (20)	94%	810 ± 50	0.8 ± 0.1
CC-L4	C6	3 (22)	2.94 ± 0.10	3.15 ± 0.30	12.2 ± 0.46	0.20 ± 0.02	4.63 ± 0.12	18.4 ± 1.32	14 (15)	25%	3,970 ± 300	4.0 ± 0.6
CC-L5	2a	4 (24)	2.60 ± 0.05	2.12 ± 0.22	11.6 ± 0.50	0.17 ± 0.01	3.98 ± 0.12	23.1 ± 1.39	18 (20)	23%	5,880 ± 390	5.9 ± 0.8
CC-L6	2bA	2 (25)	3.59 ± 0.06	2.91 ± 0.22	14.8 ± 0.47	0.18 ± 0.01	5.33 ± 0.11	18.7 ± 0.54	15 (15)	0%	3,510 ± 130	3.5 ± 0.3
CC-L7	C6A	2 (21)	2.11 ± 0.08	2.36 ± 0.27	9.71 ± 0.76	0.20 ± 0.02	3.48 ± 0.17	13.5 ± 0.45	14 (24)	28%	3,880 ± 230	3.9 ± 0.5
CC-L8	C5	2 (23)	2.59 ± 0.08	2.2 ± 0.25	12.4 ± 0.36	0.21 ± 0.02	4.10 ± 0.09	9.32 ± 0.48	10 (15)	46%	2,270 ± 110	2.3 ± 0.2
CC-L9	C4	1 (23)	2.93 ± 0.06	2.68 ± 0.25	13.2 ± 0.37	0.24 ± 0.02	4.63 ± 0.10	6.92 ± 0.46	3 (15)	40%	1,490 ± 100	1.5 ± 0.2
CC-L10	C3	1 (21)	2.75 ± 0.05	2.41 ± 0.19	13.0 ± 0.50	0.25 ± 0.02	4.40 ± 0.11	4.31 ± 0.21	9 (12)	74%	980 ± 50	1.0 ± 0.1
CC-L11	C1	1 (18)	2.19 ± 0.04	1.76 ± 0.21	10.0 ± 0.46	0.25 ± 0.02	3.52 ± 0.11	10.6 ± 1.24	9 (10)	18%	3,010 ± 360	3.0 ± 0.7
CC-L12	C2	3 (24)	2.69 ± 0.05	2.38 ± 0.21	14.1 ± 0.43	0.25 ± 0.02	4.39 ± 0.10	2.36 ± 0.13	14 (20)	94%	540 ± 30	0.5 ± 0.1
CC-L13	1d	3 (19)	2.17 ± 0.07	2.11 ± 0.26	10.8 ± 0.38	0.20 ± 0.02	3.58 ± 0.10	10.9 ± 0.79	18 (20)	26%	3,050 ± 220	3.1 ± 0.4
CC-L14	1b	1 (20)	3.38 ± 0.07	2.57 ± 0.29	13.6 ± 0.69	0.25 ± 0.02	5.10 ± 0.17	9.32 ± 0.36	6 (15)	47%	1,830 ± 90	1.8 ± 0.2
CC-L15	1a	1 (19)	2.60 ± 0.08	2.80 ± 0.28	14.0 ± 0.77	0.26 ± 0.02	4.45 ± 0.17	8.33 ± 0.32	9 (15)	43%	1,870 ± 100	1.9 ± 0.2

[1] Analyses by U.S. Geological Survey Luminescence Dating Laboratory (Denver, Colorado).

[2] Units correspond to plates 1 and 2.

[3] Field moisture percentage; complete sample saturation percent in parentheses. Ages calculated using approximately 20% of the saturated moisture.

[4] Analyses obtained using laboratory gamma spectrometry (high-resolution Ge detector).

[5] Cosmic doses and attenuation with depth were calculated using the methods of Prescott and Hutton (1994); Gy – gray.

[6] Number of replicated equivalent dose (De) estimates used to calculate the final overall equivalent dose. Figures in parentheses indicate total number of measurements included in calculating the represented equivalent dose and age using either the minimum age model (MAM) for dispersions >25% or the central age model (CAM) for dispersion <25%.

[7] Defined as "over-dispersion" of the De values. Obtained by taking the average over the standard deviation. Values >35% are considered to be poorly bleached sediments.

[8] Dose rate and age for fine-grained 150-90 micron sized quartz. Exponential fit used on equivalent doses, errors to 1σ, ages and errors rounded.

[9] Ages and uncertainties rounded to the nearest century; error to 2σ.